E6-2017-29

I. N. Izosimov, A. A. Solnyshkin,
J. H. Khushvaktov, Yu. A. Vaganov

FINE STRUCTURE OF BETA-DECAY STRENGTH FUNCTION AND ANISOTROPY OF ISOVECTOR NUCLEAR DENSITY COMPONENT OSCILLATIONS IN DEFORMED NUCLEI

Submitted to the International Conference
"Isospin, Structure, Reactions and Energy of Symmetry,"
ISTROS-2017, 14–19 May, 2017, Casta-Papiernicka, Slovakia

Изосимов И. Н. и др. Е6-2017-29

Тонкая структура силовой функции бета-распада и анизотропия осцилляций компонент изовекторной плотности в деформированных ядрах

Представлены и проанализированы экспериментальные данные о тонкой структуре силовой функции бета-распада $S_\beta(E)$ в сферических, переходных и деформированных ядрах. Использование современных методов ядерной спектроскопии с высоким энергетическим разрешением позволило идентифицировать расщепление пиков $S_\beta(E)$ в деформированных ядрах. По аналогии с расщеплением пика $E1$ гигантского дипольного резонанса (ГДР) в деформированных ядрах, пики в $S_\beta(E)$ расщепляются на две компоненты благодаря наличию аксиально-симметричной деформации атомного ядра. Обсуждается тонкая структура $S_\beta(E)$. Сравнивается расщепление пиков, связанное с колебаниями протонов относительно нейтронов ($E1$ ГДР), протонных дырок относительно нейтронов (пики в $S_\beta(E)$ для $\beta^+/$EC-распада) и нейтронных дырок относительно протонов (пики в $S_\beta(E)$ для β^--распада).

Работа выполнена в Лаборатории ядерных реакций им. Г. Н. Флерова ОИЯИ.

Препринт Объединенного института ядерных исследований. Дубна, 2017

Izosimov I. N. et al. E6-2017-29

Fine Structure of Beta-Decay Strength Function and Anisotropy of Isovector Nuclear Density Component Oscillations in Deformed Nuclei

The experimental measurement data on the fine structure of beta-decay strength function $S_\beta(E)$ in spherical, transition, and deformed nuclei are analyzed. Modern high-resolution nuclear spectroscopy methods made it possible to identify the splitting of peaks in $S_\beta(E)$ for deformed nuclei. By analogy with splitting of the peak of $E1$ giant dipole resonance (GDR) in deformed nuclei, the peaks in $S_\beta(E)$ are split into two components from the axial nuclear deformation. In this report, the fine structure of $S_\beta(E)$ is discussed. Splitting of the peaks connected with the oscillations of neutrons against protons ($E1$ GDR), of proton holes against neutrons (peaks in $S_\beta(E)$ of $\beta^+/$EC decay), and of protons against neutron holes (peaks in $S_\beta(E)$ of β^- decay) is discussed.

The investigation has been performed at the Flerov Laboratory of Nuclear Reactions, JINR.

Preprint of the Joint Institute for Nuclear Research. Dubna, 2017

INTRODUCTION

The β-decay probability is proportional to the product of the lepton part described by the Fermi function $f(Q_\beta - E)$ and the nucleon part described by $S_\beta(E)$. From the macroscopic point of view, the resonances in the Gamow–Teller (GT) β-decay strength function $S_\beta(E)$ are connected with the oscillation of the spin–isospin density without change in the shape of the nucleus [1–3]. At the nuclear excitation energies E up to Q_β (total energy of β decay), $S_\beta(E)$ determines the character of the β decay and the half-lives ($T_{1/2}$) of the β decay, spectra of β particles and neutrinos emitted in β decay, spectra of γ rays and internal conversion electrons resulting from the de-excitation of daughter nucleus states excited in the β decay, and probabilities of delayed processes accompanying the β decay [1–5]. Development of experimental technique allows application of methods of nuclear spectroscopy with high energy resolution for $S_\beta(E)$ fine structure measurement [3–5]. The combination of the total absorption spectroscopy (TAS) with high-resolution γ spectroscopy may be applied for detailed decay schemes construction [3]. High-resolution nuclear spectroscopy methods [3–5] made it possible to demonstrate experimentally the resonance nature of $S_\beta(E)$ for first-forbidden (FF) β transitions and reveal splitting of the peak in the $S_\beta(E)$ for the GT β^+/EC decay of the deformed nuclei into two components. This splitting indicates anisotropy of oscillation of the isovector nuclear density component. A low intensity component of the split peak has a larger energy and corresponds to the γ-type oscillation ($\Delta K \neq 0$) of the proton holes towards neutron particles. The other component corresponds to the β-type oscillation ($\Delta K = 0$) of the proton holes towards neutron particles. The value of such an energy splitting for GT β^+/EC decay of ^{160g}Ho is about $E_\gamma - E_\beta \approx 1$ MeV.

It is shown that the high-resolution nuclear spectroscopy methods give conclusive evidence of the $S_\beta(E)$ resonance structure for GT and FF β transitions in deformed (^{160g,160m}Ho), spherical (^{147g}Tb), and transition (^{156g}Ho) nuclei. Splitting of the peaks connected with the oscillations of neutrons against protons ($E1$ GDR), of proton holes against neutrons (peaks in $S_\beta(E)$ of the β^+/EC decay), and of protons against neutron holes (peaks in $S_\beta(E)$ of the β^- decay) is discussed.

1. BETA-DECAY STRENGTH FUNCTION $S_\beta(E)$

The strength function $S_\beta(E)$ governs the nuclear energy distribution of elementary charge-exchange excitations and their combinations like proton particle (πp) – neutron hole (νh) coupled into a momentum J^π: $[\pi p \otimes \nu h]^\pi_J$ and neutron particle (νp) – proton hole (πh) coupled into a momentum J^π: $[\nu p \otimes \pi h]^\pi_J$. The strength function of Fermi-type β transitions takes into account excitations $[\pi p \otimes \nu h]^+_0$ or $[\nu p \otimes \pi h]^+_0$. Since isospin is quite a good quantum number, the strength of the Fermi-type transitions is concentrated in the region of the isobar-analogue resonance (IAR). The strength function for β transitions of the Gamow–Teller type describes excitations $[\pi p \otimes \nu h]^+_1$ or $[\nu p \otimes \pi h]^+_1$. Significant configurations for FF β transitions in the Coulomb (ξ approximation) are $[\pi p \otimes \nu h]_{0^-,1^-}$ or $[\nu p \otimes \pi h]_{0^-,1^-}$. Residual interaction can cause collectivization of these configurations and occurrence of resonances in $S_\beta(E)$. The position and intensity of resonances in $S_\beta(E)$ are calculated within various microscopic models of the nucleus [3]. For the Gamow–Teller β transitions, FF β transitions in the ξ approximation (Coulomb approximation), and unique FF β transitions the reduced probabilities $B(\mathrm{GT})$, $[B(\lambda\pi = 0^-) + B(\lambda\pi = 1^-)]$, and $[B(\lambda\pi = 2^-)]$, half-life $T_{1/2}$, level populations $I(E)$, strength function $S_\beta(E)$, and ft values are related as follows [3]:

$$d(I(E))/dE = S_\beta(E) T_{1/2} f(Q_\beta - E), \tag{1}$$

$$(T_{1/2})^{-1} = \int S_\beta(E) f(Q_\beta - E) dE, \tag{2}$$

$$\int\limits_{\Delta E} S_\beta(E) dE = \sum_{\Delta E} 1/(ft), \tag{3}$$

$$B(\mathrm{GT}, E) = [D(g_V^2/4\pi)]/ft, \tag{4}$$

$$B(\mathrm{GT}, E) = g_A^2/4\pi \big|\langle I_f || \sum t_\pm(k)\sigma_\mu(k) || I_i\rangle\big|^2/(2I_i + 1), \tag{5}$$

$$[B(\lambda\pi = 2^-)] = 3/4[Dg_V^2/4\pi]/ft, \tag{6}$$

$$[B(\lambda\pi = 0^-) + B(\lambda\pi = 1^-)] = [Dg_V^2/4\pi]/ft, \tag{7}$$

where $D = (6147 \pm 7)$ s; Q_β is the total β-decay energy, $f(Q_\beta - E)$ is the Fermi function; t is the partial period of the β decay to the level with the excitation energy E; $1/ft$ is the reduced probability of β-decay; $\langle I_f || \sum t_\pm(k)\sigma_\mu(k) || I_i\rangle$ is the reduced nuclear matrix element for the Gamow–Teller transition; I_i is the spin of the parent nucleus; I_f is the spin of the excited state of the daughter nucleus. By measuring populations of levels in the β decay, one can find the reduced probabilities and the strength function for the beta decay. The reduced probabilities of the beta decays are proportional to the squares of the nuclear matrix elements and reflect the fine structure of the strength function for the beta

decay. For the FF β^+/EC transitions in the ξ approximation, significant configurations are the configurations like (proton hole) – (neutron particles) coupled into the momentum 0^- or 1^-: $[\nu p \otimes \pi h]_{0^-,1^-}$.

Information on the structure of $S_\beta(E)$ is important for many nuclear physics areas [1–3]. Reliable experimental data on the structure of $S_\beta(E)$ are necessary for predicting half-lives of nuclei far from the stability line, verifying completeness of decay schemes, calculating energy release from decay of fission products in nuclear reactors, calculating spectra of delayed particles, calculating the delayed fission probability and evaluating fission barriers for nuclei far from the β-stability line, calculating production of various elements in astrophysical processes, and developing microscopic models for calculation of $S_\beta(E)$, especially in deformed nuclei.

Until recently, experimental investigations of the $S_\beta(E)$ structure were carried out using total absorption gamma-ray spectrometers (TAGS) and total absorption spectroscopy methods, which had low energy resolution. In the TAGS technique, the γ radiation accompanying the β decay is summarized by employing large NaI crystals for its detection in the 4π-geometry. If the efficiency of the total γ-ray absorption is sufficiently high, total absorption peaks with an intensity governed only by the probability for population of levels in β decay can be identified in the spectra. This approach has allowed the resonance structure of $S_\beta(E)$ for GT β transitions to be experimentally proved [2]. It was found that the resonance structure of $S_\beta(E)$ is a typical feature of the GT β decay of nuclei far from the β-stability line [2]. The previously dominant statistical model assumed that there were no resonances in $S_\beta(E)$ and the relations $S_\beta(E) = \mathrm{const}$ or $S_\beta(E) \sim \rho(E)$, where $\rho(E)$ is the level density of the daughter nucleus, were considered to be good approximations for medium and heavy nuclei for excitation energies $E > 2{-}3$ MeV [6]. TAGS investigations unambiguously revealed the nonstatistical character of $S_\beta(E)$ for the GT-type β decay and stimulated development of microscopic models making it possible to use the structure of the atomic nucleus for calculating $S_\beta(E)$ [1–5, 7]. However, TAGS methods have some disadvantages arising from poor energy resolution of NaI-based spectrometers. Only one or two absorption peaks can be identified in TAGS spectra, isobaric impurities in the analyzed source often give rise to uncertainties, it is impossible to discriminate between GT and FF β transitions and to measure the fine structure of $S_\beta(E)$; difficulties often emerge in spectrum processing, such as when one has to take into account internal conversion of γ rays or to identify total absorption peaks. Exponential dependence [2, 3] of the TAGS efficiency on the energy is substantially important for the total absorption spectrometer and requires experimental verification in the range of energies up to Q_β. Therefore, it is quite important to measure $S_\beta(E)$ using high-resolution γ-spectroscopy techniques. It is a rather arduous task, and no measurements of this kind had been performed until recently. Only in the past

decade, with great advances in production of monoisotopic radioactive sources and the advent of semiconductor HPGe γ-ray detectors combining high energy resolution and adequate efficiency, it has become possible to measure $S_\beta(E)$ with high confidence and high energy resolution. This allows thorough investigation of $S_\beta(E)$ at a qualitatively new level [3]. JINR (Dubna) was the first to use high-resolution nuclear spectroscopy techniques to rather fully determine the function $S_\beta(E)$ and its fine structure. It is a rather laborious problem that was solved only for the β^+/EC decay of the spherical nucleus ^{147g}Tb ($T_{1/2} = 1.6$ h, $Q_{\mathrm{EC}} = 4.6$ MeV), deformed nucleus ^{160g}Ho ($T_{1/2} = 25.6$ min, $Q_{\mathrm{EC}} = 3.3$ MeV), and isomer ^{160m}Ho ($T_{1/2} = 5.02$ h, $Q_{\mathrm{EC}} = 3346$ keV) [3]. These nuclei were chosen for investigation because of their rather large Q_{EC}, suitable half-lives $T_{1/2}$, and the possibility of effectively producing high-purity monoisotopic radioactive sources of those nuclei at JINR. In this work, data on the structure of $S_\beta(E)$ for β^+/EC decay of the transition nuclei ^{156g}Ho ($T_{1/2} = 56$ min, $Q_{\mathrm{EC}} = 5.05$ MeV) were obtained using nuclear spectroscopy methods of high energy resolution.

These high-resolution nuclear spectroscopy techniques made it possible to unambiguously demonstrate the resonance structure of $S_\beta(E)$, not only for GT β transitions but also for FF β transitions [3–5]. It was experimentally shown that for some excitation energies of daughter nuclei, the probability of the first forbidden β^+/EC transitions is comparable with the probability of the GT β^+/EC transitions. It is due to high-resolution spectroscopy techniques that the resonance structure of $S_\beta(E)$ for FF transitions was first revealed [3–5].

By analogy with splitting of the peak of $E1$ giant resonance (GDR) [8–10] in deformed nuclei, the peaks in $S_\beta(E)$ are split into two components from the axial nuclear deformation [3]. In this work, such a splitting and its connection with anisotropy of the isovector spin–isospin oscillation in deformed nuclei are discussed.

2. $S_\beta(E)$ FOR THE GT β^+/EC DECAY OF THE TRANSITION NUCLEI ^{156g}Ho

In our experiments, we produced radioactive ^{156}Ho using the reaction of deep spallation of tantalum nuclei bombarded by high-energy protons from the Phasotron (FLNP, JINR) [3, 11]. To this end, a metal tantalum target with the mass of 5 g was inserted with a special device into the Phasotron chamber without vacuum deterioration. Then the target was irradiated by a proton beam. The irradiation time varied from a few tens of minutes to a few hours. In all irradiation runs, the proton energy was $E_p = 660$ MeV, and the intensity was $I_p = 2$ μA. After irradiation the target was removed from the accelerator chamber and delivered to the radiochemical laboratory, where the Ho fraction was

separated with the chromatographic method [12]. The total time from the removal of the target till the end of the Ho fraction separation was no longer than two hours. Then the Ho fraction was transported to the YASNAPP-2 electromagnetic mass separator [13], where it was placed into a special ion source ampoule and separated into particular Ho isotopes. Mass resolution of YASNAPP-2 was $M/\Delta M = 1500$. In a special collector, the monoisotopes in the form of ions with the energy of 50 keV were deposited (each in its own place) on an aluminum tape. The tape was removed from the collector and cut into separate fragments about 1 cm^2 in size with a specific monoisotope. These fragments, including those with ^{156g}Ho, were later used as radioactive sources for measurements with our semiconductor spectrometers. The entire separation process up to the beginning of the measurements was no longer than an hour. Thus, the total time from the end of irradiation till the beginning of measurements was about three hours. In this time, the 8-min (9^+) ^{156m}Ho isomer almost completely decayed, and we measured gamma spectra from the decay of the (4^-) ^{156g}Ho (56 min) ground state. The measurements were performed using spectrometers based on standard ORTEC and CANBERRA HPGe detectors. Spectra of both γ rays and $\gamma\gamma t$ coincidences in the ^{156g}Ho (56 min) decay were measured. The characteristics of the detectors used in our measurements are given below.

Efficiency:	Resolution:
HPGe (19%)	$\Delta E_\gamma = 1.8$ keV (^{60}Co)
HPGe (28%)	$\Delta E_\gamma = 1.9$ keV (^{60}Co)
HPGe (50%)	$\Delta E_\gamma = 2.0$ keV (^{60}Co)
HPGe (2 cm^3)	$\Delta E_\gamma = 580$ eV at $E_\gamma = 120$ keV

Total absorption gamma spectra were also measured using the TAGS spectrometer with the characteristics given in [3, 11].

In [14], which was published in 2002, the authors performed γ spectroscopy of the ^{156}Er $\rightarrow$ ^{156}Ho $\rightarrow$ ^{156}Dy decay chain using the Clover HPGe detector. The ^{156}Er source was produced via the ^{148}Sm(^{12}C, $4n$)^{156}Er reaction in the ^{12}C beam with the energy of 73 MeV. Our data on the γ rays (energies and intensities) and $\gamma\gamma t$ coincidences in the ^{156g}Ho (56 min) decay are in good agreement within the errors with the data [14], except for the 137.8-keV γ transition from the 2_1^+ state to the 0_1^+ ground state of ^{156}Dy. According to our data, its intensity in relative units is $I_\gamma = 115.0 \pm 3.0$, while in [14] it is slightly underestimated, $I_\gamma = 100 \pm 7$.

In this work, using our data (Table 1) and data from [14], we succeeded in estimating (Fig. 1) the strength function $S_\beta(E)$ for the β^+/EC decay of the ^{156g}Ho (56 min) nucleus.

Since there are no sufficient data for finding the fine structure of $S_\beta(E)$ at the ^{156}Dy excitation energies above 3 MeV, Fig. 1 presents $S_\beta(E)$ in relative units. At the excitation energies of 2.8 MeV, the resonance is observed in $S_\beta(E)$.

Table 1. ^{156}**Dy levels excited by the** $\varepsilon + \beta^+$ **decay** ^{156g}**Ho** $\rightarrow$ ^{156}**Dy**

$E_{\rm level}(\Delta E_{\rm level})$, keV	Quantum characteristics ($I^\pi K^\pi$)	Level population from the $\varepsilon + \beta^+$ decay, % per decay	Type of transition	lg ft
137.77(8)	2^+0	6.82(31)	1U	9.32(19)
404.19(10)	4^+0	10.46(37)	FF	7.34(18)
675.60(14)	0^+0	0.03(6)		
770.44(11)	6^+0	6.11(12)	1U	9.04(10)
828.64(11)	2^+0	2.12(4)	1U	9.46(1)
890.50(9)	2^+2	2.19(44)	1U	9.41(8)
1022.08(10)	3^+2	2.57(14)	FF	7.7(3)
1088.28(11)	4^+0	6.41(86)	FF	7.24(7)
1168.47(11)	4^+2	4.72(33)	FF	7.33(3)
1215.61(20)	8^+0	(0.05(2))	(3U)	
1335.56(13)	5^+2	2.14(40)	FF	7.61(09)
1368.36(12)	3^-0	2.96(12)	GT	7.44(2)
1382.31(16)	2^+	1.35(4)	1U	9.34(1)
1437.28(17)	6^+0	2.80(10)	1U	8.99(2)
1476.10(15)	$(3)^-$	0.60(8)	(GT)	8.09(6)
1514.94(20)	2^+	0.38(8)	1U	9.81(10)
1525.17(19)	6^+2	2.43(3)	1U	9.00(1)
1526.28(20)	5^-0	3.38(8)	GT	7.31(1)
1609.33(16)	$(3)^-$	1.73(24)	(GT)	7.57(6)
1624.64(18)		0.65(2)		
1627.42(16)	$(4)^+$	2.46(19)	(FF)	7.41(4)
1656.07(8)*		0.17(5)		
1677.15(15)	4^+	0.7(1)	FF	7.93(7)
1679.9(8)		0.39(8)		
1728.79(12)	7^+2	0.14(4)		
1772.4(10)	(3^-)	0.50(14)	(GT)	8.03(13)
1794.55(19)	4^+	1.00(6)	FF	7.72(3)
1809.97(10)	7^-0	0.18(3)	2U	11.51(10)
1840.07(13)	(4^+)	0.78(6)	(FF)	7.81(4)
1857.84(14)		1.13(15)		
1876.09(10)*		0.10(6)		
1878.6(4)	$(2)^+$	0.53(8)	(1U)	9.44(7)

Table 1 (continued)

$E_{\rm level}(\Delta E_{\rm level})$, keV	Quantum characteristics $(I^{\pi}K^{\pi})$	Level population from the $\varepsilon + \beta^{+}$ decay, % per decay	Type of transition	lg ft
1898.64(10)	6^{-}	0.47(4)		
1930.1(5)	(3^{-})	0.52(11)	(GT)	7.94(10)
1933.60(18)		0.69(8)		
1942.9(4)		0.43(8)		
1949.99(22)	(3^{-})	0.66(4)	(GT)	7.83(3)
2002.9(3)	4^{+}	0.28(5)	FF	8.18(8)
2047.24(11)*		0.05(2)		
2058.49(20)		0.26(7)		
2085.14(23)		0.24(3)		
2089.81(22)	2^{+}	0.57(8)	1U	9.27(6)
2103.38(25)	(4^{+})	0.40(4)	(FF)	8.07(13)
2138.49(10)*		0.31(9)		
2161.99(10)*		0.12(4)		
2164.3(5)		0.18(4)		
2178.87(8)*		0.15(4)		
2183.7(5)		0.20(5)		
2191.64(11)*		0.05(2)		
2193.6(3)	4^{+}	0.23(4)	FF	8.18(8)
2199.68(19)		0.48(8)		
2202.37(8)*		0.06(4)		
2207.4(4)		0.18(3)		
2220.4(4)		0.10(3)		
2228.9(5)		0.29(4)		
2230.9(4)		0.10(2)		
2244.64(14)	(3^{-})	1.52(9)	(GT)	7.33(3)
2264.3(5)		0.52(7)		
2270.0(4)		0.28(4)		
2271.79(10)*		0.14(4)		
2293.4(4)		0.34(5)		
2300.1(4)		0.13(2)		
2302.99(10)*		0.15(4)		
2307.44(12)	4^{+}	1.62(10)	FF	7.28(3)
2323.58(13)		3.03(12)		

Table 1 (continued)

$E_{\mathrm{level}}(\Delta E_{\mathrm{level}})$, keV	Quantum characteristics $(I^{\pi}K^{\pi})$	Level population from the $\varepsilon + \beta^{+}$ decay, % per decay	Type of transition	lg ft
2331.7(3)		0.28(5)		
2342.68(23)		0.19(4)		
2355.68(15)*		0.06(2)		
2363.89(10)*		0.11(4)		
2372.1(3)		1.04(19)		
2374.16(13)*		0.05(2)		
2385.7(3)		0.20(4)		
2393.39(10)*		0.14(7)		
2403.94(11)*		0.08(3)		
2408.45(14)	2^{+}, 3, 4^{+}	1.24(10)	FF	7.35(4)
2412.44(11)*		0.17(8)		
2413.09(10)*		0.12(4)		
2415.17(8)*		0.19(6)		
2419.1(6)		0.19(4)		
2424.44(11)*		0.06(3)		
2428.44(11)*		0.06(3)		
2433.84(16)		1.40(10)		
2439.16(17)		0.96(1)		
2441.67(8)		0.10(4)		
2445.17(21)	3^{+}, 4^{+}	0.70(7)	FF	7.58(5)
2474.44(11)*		0.04(2)		
2482.04(11)*		0.06(2)		
2489.5(5)		0.33(7)		
2491.90(18)		0.74(9)		
2503.44(11)*		0.10(3)		
2514.96(13)*		0.12(4)		
2517.0(4)		0.4(2)		
2528.34(11)*		0.04(4)		
2534.56(13)*		0.10(3)		
2539.79(10)*		0.20(5)		
2545.16(12)*		0.04(2)		
2571.7(5)		0.17(4)		
2594.3(3)		0.24(5)		

Table 1 (continued)

$E_{\rm level}(\Delta E_{\rm level})$, keV	Quantum characteristics $(I^\pi K^\pi)$	Level population from the $\varepsilon + \beta^+$ decay, % per decay	Type of transition	lg ft
2642.50(22)		0.35(7)		
2653.3(6)		0.24(7)		
2677.72(16)*		0.035(17)		
2690.49(10)*		0.12(4)		
2710.89(10)*		0.15(5)		
2729.54(11)*		0.035(17)		
2732.24(11)*		0.026(17)		
2743.39(10)*		0.08(4)		
2757.8(6)		0.08(3)		
2759.64(11)*		0.04(7)		
2771.98(15)*		0.06(3)		
2788.1(9)		0.035(9)		
2810.4(7)		0.23(5)		
2818.35(12)	4^+, 5^-	3.42(14)	GT	6.72(2)
2823.38(15)		2.16(16)	GT	6.91(4)
2833.7(4)		0.39(4)		
2848.96(12)		0.10(3)		
2865.68(10)*		0.035(17)		
2885.59(10)*		0.08(2)		
2895.0(4)		0.24(4)		
2962.74(11)*		0.04(2)		
2981.5(13)		0.15(4)		
3195.49(20)*		0.10(4)		
3222.7(2)*		0.07(3)		
3350.24(11)*		0.035(17)		
3361.24(11)*		0.026(1)		
3383.84(11)*		0.04(1)		
		$\sum = 101(5)\%$		

Note. * are excited ^{156}Dy states first established in this work.

The total absorption gamma spectrum (TAGS) (Fig. 2) also indicates presence of a peak in $S_\beta(E)$ in the above-mentioned region of excitation energies. There is a distinct peak in $S_\beta(E)$ at the excitation energy of $2.3 < E < 3$ MeV. The solid distribution at $E > 3$ MeV leads to a contribution from the incomplete

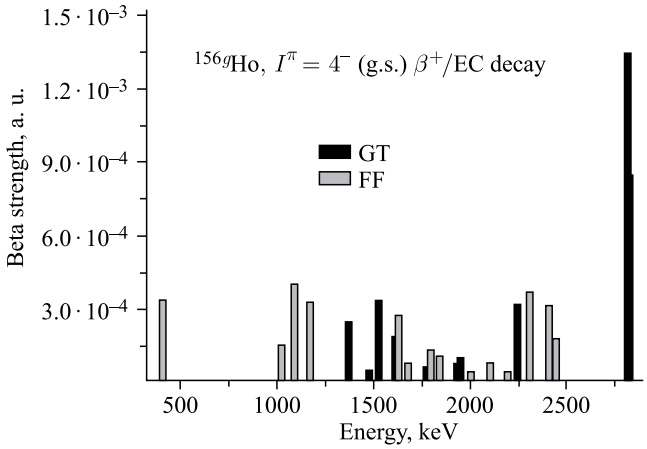

Fig. 1. Structure of the strength function for the GT β^{+}/EC decay of transition nuclei ^{156g}Ho ($Q_{\mathrm{EC}} = 5.05$ MeV)

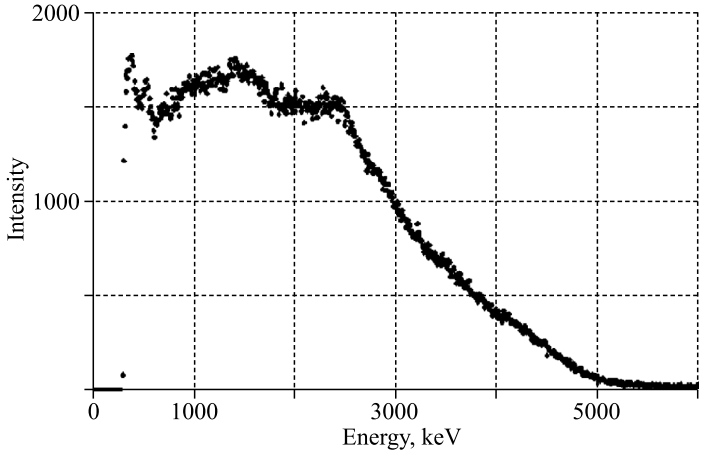

Fig. 2. TAGS spectra of ^{156g}Ho [11]

summation of gamma cascades to the total absorption peak in the region of $2.3 < E < 3$ MeV, which can cause a shift of the maximum of this peak and makes it difficult to obtain information on the $S_{\beta}(E)$ structure from the TAGS analysis.

Joint analysis of the TAGS and the spectra obtained by nuclear spectroscopy methods with higher energy resolution allows the following conclusions to be drawn. The peaks in the TAGS contain not only total absorption components

but also a contribution from the cascades with incomplete summation of gamma cascades and can provide only qualitative information on the $S_\beta(E)$ structure. The $S_\beta(E)$ for the GT β^+/EC decay of the ^{156g}Ho transition nuclei have a resonant character, and the resonance(s) in ^{156}Dy is / are at the excitation energy above 2.8 MeV. Since the data on the decay scheme at energies above 3 MeV are unavailable or tentative, only qualitative estimates in relative units can be obtained for the fine structure of $S_\beta(E)$. The fine structure of $S_\beta(E)$ (Fig. 1) does not contradict the TAGS spectroscopy data (Fig. 2).

3. SPLITTING OF THE PEAKS IN $S_\beta(E)$ FOR BETA DECAY OF DEFORMED NUCLEI

From the macroscopic point of view, the resonances in the GT β-decay strength function $S_\beta(E)$ are connected with the oscillation of the spin–isospin density without change in the shape of the nucleus [2]. Data on the population of levels in ^{160}Dy by the ^{160g}Ho β^+/EC decay are presented in [3, 15] and Table 2. Data on the most intense components of the $S_\beta(E)$ peaks for the ^{160g}Ho GT β^+/EC decay are presented in Tables 3 and 4.

Table 2. Levels of ^{160}Dy [3, 15], populated by the β^+/EC decay of ^{160g}Ho (25.6 min), $I^\pi = 5^+$, $K^\pi = 5^+$

Energy of the level, keV	Quantum characteristics $(I^\pi; K^\pi)$	Level population from the $\varepsilon + \beta^+$ decay, % per decay	$\lg ft$
1386.46(2)	$I^\pi = 4^-$; $K^\pi = 2^-$	0.27(3)	7.32(5)
1438.57(3)	$I^\pi = 6^+$; $K^\pi = 2^+$	0.2(1)	7.4(2)
1535.14(2)	$I^\pi = 4^-$; $K^\pi = 4^-$	0.11(2)	7.63(8)
1603.77(8)	$I^\pi = 4^+$; $K^\pi = (4^+)$	0.07(2)	7.8(1)
1606.9(1)	$I^\pi = 6^+$; $K^\pi = (6^+)$	0.10(1)	7.63(5)
1607.9(1)	$I^\pi = 4^+ S$	0.08(2)	7.7(1)
1650.87(4)	$I^\pi = 4^-, 5^-$; $K^\pi = (4^-, 5^-)$	0.02(1)	8.3(2)
1652.1(1)	$I^\pi = (4, 5, 6)^+$; $K^\pi = (4, 5, 6)^+$	0.16(2)	7.41(6)
1694.36(2)	$I^\pi = 4^+$; $K^\pi = 4^+$	74(5)	4.72(3)
1802.24(2)	$I^\pi = 5^+$; $K^\pi = 4^+$	10.8(9)	5.49(4)
1860.1(1)	$I^\pi = 5^-$; $K^\pi = 4^-$	0.11(1)	7.44(4)
1929.19(2)	$I^\pi = 6^+$; $K^\pi = 4^+$	0.62(7)	6.65(5)
2096.87(2)	$I^\pi = 4^+$; $K^\pi = 4^+$	2.9(2)	5.86(3)
2143.7(1)	$I^\pi = (4^-)$; $K^\pi = (4^-)$	0.13(2)	7.17(7)
2155.3(2)	$I^\pi = (4^-)$	0.035(3)	7.73(4)

Table 2 (continued)

Energy of the level, keV	Quantum characteristics $(I^\pi; K^\pi)$	Level population from the $\varepsilon + \beta^+$ decay, % per decay	lg ft
2187.0(1)	$I^\pi = (4,5,6)^+$; $K^\pi = (4,5,6)^+$	0.09(1)	7.30(5)
2194.43(3)	$I^\pi = 5^+$; $K^\pi = 4^+$	0.43(3)	6.61(4)
2208.4(1)	$I^\pi = 4^+$; $K^\pi = 2^+$	0.20(3)	6.93(7)
2374.5(1)	$I^\pi = (4^-)$	0.036(5)	7.52(7)
2556.8(1)	$I^\pi = 5^-$; $K^\pi = 5^-$	0.14(2)	6.73(7)
2572.4(1)	$I^\pi = (3,4,5)^+$; $K^\pi = (3,4,5)^+$	0.032(3)	7.35(5)
2681.9(1)	$I^\pi = 5^+$; $K^\pi = 2^+$	0.8(1)	5.80(6)
2727.2(1)	$I^\pi = (4)$	0.037(5)	7.06(7)
2755.0(2)	$I^\pi = (4^-)$	0.027(4)	7.15(7)
2757.1(1)		0.040(7)	6.97(8)
2763.0(1)		0.07(1)	6.72(7)
2777.6(1)	$I^\pi = (2,3,4)^+$; $K^\pi = (2,3,4)^+$	0.29(2)	6.07(5)
2853.6(1)		0.055(6)	6.64(6)
2941.7(1)	$I^\pi = (4,5,6)$	0.023(2)	6.79(6)
2969.9(1)		0.06(2)	6.3(2)
2977.5(1)		0.021(5)	6.7(1)
3033.7(2)		0.0031(9)	7.3(2)
3081.4(2)		0.0024(7)	7.2(2)

The average energy $\langle E \rangle$ of the $S_\beta(E)$ peak is calculated by the formula

$$\langle E \rangle = \frac{\sum\limits_i E_i \times ft_i^{-1}}{\sum\limits_i ft_i^{-1}}. \tag{8}$$

Using the data from Table 3, we obtain $\langle E \rangle_\beta = 1749$ keV.

Intensities of K-allowed β transitions to the levels of the same rotational band and intensity ratios of electromagnetic transitions inside the band and between states of different bands satisfy simple relations following from the rotational model (Alagi rules) [16]. The ft ratios at $|K_i - K_f| \leqslant \lambda$ and $|K_i + K_f| > \lambda$ are expressed in terms of the ratios of the squares of the corresponding Clebsch–Gordan coefficients:

$$\frac{ft(I_i K_i \to I_{1f} K_f)}{ft(I_i K_i \to I_{2f} K_f)} = \frac{\langle I_i K_i \lambda K_i - K_f | I_{2f} K_f \rangle^2}{\langle I_i K_i \lambda K_i - K_f | I_{1f} K_f \rangle^2}, \tag{9}$$

Table 3. ^{160}Dy levels populated by the ^{160g}Ho (25.6 min) GT β^+/EC decay and making the largest contribution to the intensity of the β component of the $S_\beta(E)$ peak

Energy of the level, keV	Quantum characteristics $(I^\pi; K^\pi)$	Level population from the $\varepsilon + \beta^+$ decay, % per decay	lg ft
1694.36(2)$\hat{}\hat{}$	$I^\pi = 4^+$; $K^\pi = 4^+$	74(5)	4.72(3)
1802.24(2)$\hat{}\hat{}$	$I^\pi = 5^+$; $K^\pi = 4^+$	10.8(9)	5.49(4)
1929.19(2)$\hat{}\hat{}$	$I^\pi = 6^+$; $K^\pi = 4^+$	0.62(7)	6.65(5)
2096.87(2)*	$I^\pi = 4^+$; $K^\pi = 4^+$	2.9(2)	5.86(3)
2194.43(3)*	$I^\pi = 5^+$; $K^\pi = 4^+$	0.43(3)	6.61(4)
Note. * and $\hat{}\hat{}$ are the levels in the same rotational bands.			

where λ is the β transition multipolarity ($\lambda = 1$ for GT β transitions). If $|K_i + K_f| \leqslant \lambda$ and $K_{i,f} \neq 0$, contributions from the signature-involving terms must be taken into account [8]. Obeyance of this rule means that the wave functions of the rotational band levels do not have impurity components of neighboring states and the adiabaticity condition is fulfilled. The results of the calculations by formula (9) and the experimental data are presented in Table 4.

Table 4. Ratios of ft for pairs of levels from the same band populated by the ^{160g}Ho (25.6 min) GT β^+/EC decay, $I^\pi = 5^+$, $K^\pi = 5^+$. Experimental and calculated data are given for two rotational bands in ^{160}Dy

Energy of the level E_1, keV	Energy of the level E_2, keV	Experiment, $ft(E_1)/ft(E_2)$	Calculation by formula (9), $ft(E_1)/ft(E_2)$
1694.2	1802.2	0.16	0.11
1694.2	1929.1	0.012	0.018
1802.2	1929.1	0.07	0.16
2096.8	2194.4	0.17	0.11

Considering the excitation energy and quantum characteristic of the levels, experimental data are in rather good agreement (Table 4) with the estimations by (9), which indicates correct balance of the ^{160g}Ho (25.6 min) decay scheme.

Using the data from Table 5, we obtain $\langle E\rangle_\gamma = 2737$ keV. Thus, the splitting due to the anisotropy of the spin–isospin density oscillations $\langle E\rangle_\gamma - \langle E\rangle_\beta$ in the deformed ^{160}Dy nucleus is about 1 MeV.

High-resolution nuclear-spectroscopy methods allowed observing two-component splitting of the resonance in $S_\beta(E)$ for the GT β^+/EC decay of the deformed ^{160g}Ho nucleus. This splitting is about 1 MeV. It is associated with anisotropy

Table 5. ^{160}Dy levels populated by the ^{160g}Ho (25.6 min) GT β^+/EC decay and making the largest contribution to the intensity of the γ component of the $S_\beta(E)$ peak

Energy of the level, keV	Quantum characteristics $(I^\pi; K^\pi)$	Level population from the $\varepsilon + \beta^+$ decay, % per decay	$\lg ft$
2208.4(1)*	$I^\pi = 4^+;\ K^\pi = 2^+$	0.20(3)	6.93(7)
2681.9(1)*	$I^\pi = 5^+;\ K^\pi = 2^+$	0.8(1)	5.80(6)
2777.6(1)	$I^\pi = (2,3,4)^+;\ K^\pi = (2,3,4)^+$	0.29(2)	6.07(5)
2969.9(1)		0.06(2)	6.3(2)
Note. * are the levels in the same rotational band.			

of spin–isospin oscillations in deformed nuclei [3]. When the oscillations are along the symmetry axis (β-type oscillations), the projection of the momentum on the axis is zero ($\Delta K = 0$), the axial symmetry is not broken, and oscillations of this type do not lead to K-forbidding for GT beta transitions. Oscillations perpendicular to the symmetry axis (γ-type oscillations) break the axial symmetry and have a nonzero projection of the momentum on the axis ($\Delta K = \pm 1$ for dipole oscillations, $\Delta K = \pm 2$ for quadrupole oscillations, etc.), which leads to K-forbidding for a number of β^+/EC transitions and a decrease in the intensity of the corresponding component of the peak in $S_\beta(E)$ (Fig. 3). A significant fact is that the amplitude of the higher-energy peak is much smaller than the amplitude of the lower-energy peak. This relationship of the peak amplitudes arises from

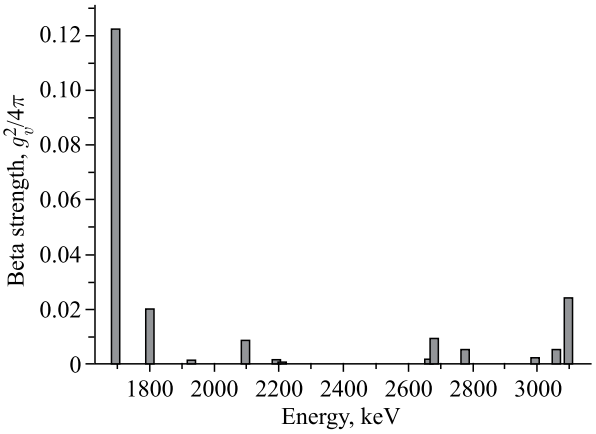

Fig. 3. Structure of the strength function [3] for the GT β^+/EC decay of deformed nuclei ^{160g}Ho

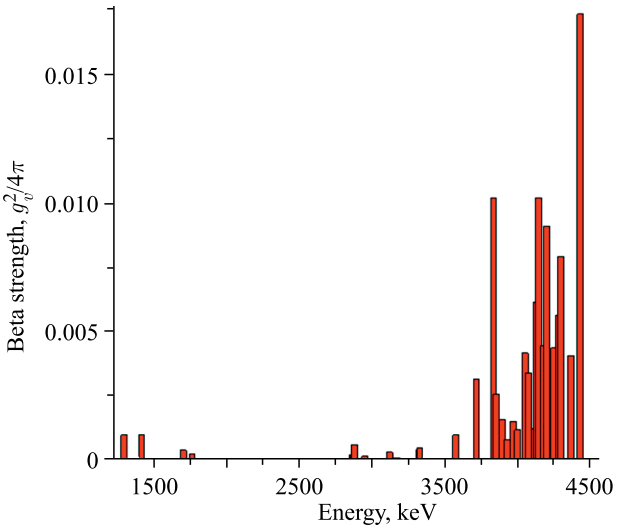

Fig. 4. Structure of the strength function [3] for the GT β^+/EC decay of spherical nuclei ^{147g}Tb

K-forbidding of GT transitions for a prolate nucleus (quadrupole deformation parameter $\beta_2 > 0$).

No similar splitting of the peak (Fig. 4) in $S_\beta(E)$ is observed in the GT β^+/EC decay of the spherical ^{147g}Tb nucleus [3]. Slight splitting of the peak in $S_\beta(E)$ for ^{147g}Tb gives comparable intensities of the components and is related to the so-called configurational splitting [17].

As a rule, theory describes positions and relative intensities of peaks for spherical nuclei quite well, but it overestimates reduced probabilities of the beta decay and is confined to the description of only spherical and transition nuclei [3].

4. DISCUSSION AND RESULTS

Isoscalar quadrupole oscillations of protons and neutrons in deformed nuclei along the symmetry axis (β vibrations) and perpendicular to it (γ vibrations) are quite well studied for a wide range of nuclei. Difference in the energies of the β type and γ type vibrations are in the range of several hundred keV and depends on nuclear structure (240 keV for ^{160}Dy and 378 keV for ^{150}Nd, the quadrupole deformation parameters are $\beta_2 = 0.33$ for ^{160}Dy and $\beta_2 = 0.29$ for ^{150}Nd) [15].

In deformed nuclei, splitting of the giant dipole resonance (GDR) into two components is observed, and the frequency difference of the isovector dipole oscillations of protons relative to neutrons perpendicular and along the symmetry

axis is several MeV (about 3 MeV for ^{150}Nd [15]). The following semi-empirical relation was proposed for a more accurate description of the GDR position [9, 10]:

$$E_{\max} \approx 31.2A^{-1/3} + 20.6A^{-1/6} \text{ MeV}. \tag{10}$$

Positions of two GDR peaks can be estimated using the model of the harmonic oscillator with axial symmetry, and they depend on the nuclear quadrupole deformation parameter β_2:

$$E_{\max 1} \approx E_{\max}/(1 - 1/3\beta_2), \tag{11}$$

$$E_{\max 2} \approx E_{\max}/(1 + 2/3\beta_2). \tag{12}$$

To the lower-energy peak there correspond oscillations along the major axis of the nuclear ellipsoid, and to the higher-energy peak there correspond those along the minor axis. In ^{150}Nd with the deformation parameter $\beta_2 = 0.29$ the GDR is seen to split into two components with the peaks at the energies of 12.5 and 15.5 MeV [9, 10].

Charge-exchange particle–hole excitations populated by the β decay are related to the oscillation of the $\mu_\tau = \pm 1$ components of the isovector density [3] $\rho_{\tau=1,\mu\tau}$:

$$\rho_{\tau=1,\mu\tau}(r) = \sum_k 2\mathbf{t}_{\boldsymbol{\mu\tau}}(k)\delta(r - r_k), \tag{13}$$

where summation is taken over all nucleons k, $\mathbf{t}_{\boldsymbol{\mu\tau}}$ is the spherical component of the nucleon isospin $\mathbf{t}$.

$$t_{\mu\tau} = \begin{cases} (1/2)^{1/2}(t_x - it_y), & \mu_\tau = -1, \\ t_z, & \mu_\tau = 0, \\ -(1/2)^{1/2}(t_x + it_y), & \mu_\tau = +1. \end{cases} \tag{14}$$

Oscillations with $\tau = 0$ correspond to oscillation of the isoscalar (total) density. Oscillations with $\tau = 1$, $\mu_\tau = 0$, $I^\pi = 1^-$ correspond to the oscillation of the $\rho_{\tau=1,0}$ component of the isovector density and describe oscillation of protons and neutrons moving in antiphase (oscillations of neutrons agaist protons), and deformation leads to splitting of the $E1$ giant resonance (GDR) peak [8–10]. Oscillations with $\tau = 1$, $\mu_\tau = \pm 1$ describe β^+/EC (oscillations of proton holes against neutrons) and β^- decays (oscillations of protons against neutron holes), and the peaks in the strength functions for deformed nuclei should also be split [2, 3].

In this study, we experimentally observed splitting of the peak in the strength function for the Gamow–Teller β^+/EC decay of the deformed ^{160g}Ho nucleus, which corresponds to oscillation anisotropy of the isovector density component

$\rho_{\tau,\mu=1,1}$. Anisotropy of the spin–isospin density oscillations results in the difference of oscillation energies $\langle E\rangle_\gamma - \langle E\rangle_\beta$ of proton holes against neutron particles perpendicular to the symmetry axis and along symmetry axis, which in the deformed ^{160}Dy nucleus is about 1 MeV. The isovector density oscillation amplitudes are tensors not only in isospace and orbital space, which leads to splitting of the $E1$ resonance in deformed nuclei, but also in spin space, which leads to splitting of the peaks in $S_\beta(E)$ in deformed nuclei (Fig. 3).

Acknowledgements. The authors are grateful to Professor V. G. Kalinnikov for interesting discussions about the subjects of this paper.

REFERENCES

1. *Izosimov I. N., Naumov Yu. V.* Influence of the Strength Function of β-Transitions on the Probability of Delayed Fission of ^{236}U and ^{238}U // Bull. Acad. Sci. USSR, Phys. Ser. 1978. V. 42, No. 11. P. 25–32.
2. *Naumov Yu. V., Bykov A. A., Izosimov I. N.* Structure of β-Decay Strength Functions // Sov. J. Part. Nucl. 1983. V.14, No. 2. P.175–200.
3. *Izosimov I. N., Kalinnikov V. G., Solnyshkin A. A.* Fine Structure of Strength Functions for Beta Decays of Atomic Nuclei // Phys. Part. Nucl. 2011. V. 42, No. 6. P. 963–997.
4. *Izosimov I. N., Kalinnikov V. G., Solnyshkin A. A.* Resonance Structure of Strength Functions for First-Forbidden β^+/EC Transitions // Phys. At. Nucl. 2012. V. 75. P. 1324–1330.
5. *Izosimov I. N., Kalinnikov V. G., Solnyshkin A. A.* Resonance Structure of the Gamow–Teller (GT) and First Forbidden (FF) β^+/EC Decay Strength Functions // J. Phys.: Conf. Ser. 2012. V. 381. P. 012054.
6. *Hansen P. G.* The Beta Strength Function // Adv. Nucl. Phys. 1974. V. 7. P. 159–170.
7. *Izosimov I. N.* Manifestations of Nonstatistical Effects in Nuclei // Phys. Part. Nucl. 1999. V. 30, No. 2. P. 131–155.
8. *Bohr A., Mottelson B.* Nuclear Structure. V. 2. New York: Benjamin, 1974.
9. *Ishkhanov B. S., Orlin V. N.* A Semimicroscopic Description of the Dipole Giant Resonance // Phys. Part. Nucl. 2007. V. 38, No. 2. P. 232–254.
10. *Masur V. M., Mel'nikova L. M.* Giant Dipole Resonance in Absorption and Emission of γ-Rays by Medium and Heavy Nuclei // Phys. Part. Nucl. 2006. V. 37, No. 6. P. 923–940.
11. *Izosimov I. N., Kazimov A. A., Kalinnikov V. G., Solnyshkin A. A.* Determination of the Total Energy Q_{EC} for ^{156}Ho ($T_{1/2} \sim 56$ min) β^+/EC Decay Using the Total Absorption γ-Ray Spectrometer // Part. Nucl. Lett. 2002. V. 2. P. 36–38.
12. *Molnar F., Khalkin V. A., Herrman E.* Production of High-Radioactivity Specimens of Neutron Deficient Isotopes of Rare Earth Elements for Nuclear Spectroscopy Purposes // Sov. J. Part. Nucl. 1973. V. 4, No. 4. P. 440–467.

13. *Kalinnikov V. G., Gromov K. Ya., Janicki M., Yushkevich Yu. V., Potempa A. W., Egorov V. G., Bystrov V. A., Kotovsky N. Yu., Evtisov S. V.* Experimental Complex to Study Nuclei Far from the Beta-Stability Line — ISOL-Facility YASNAPP-2 // Nucl. Instr. Meth. 1992. V. B70. P. 62–68.

14. *Caprio M. A., Zamfir N. V., Casten R. F., Barton C. J., Beausang C. W., Cooper J. R., Hecht A. A., Krucken R., Newman H., Novak J. R., Pietralla N., Wolf A., Zyromski K. E.* Low-Spin Structure of ^{156}Ho through γ-Ray Spectroscopy // Phys. Rev. 2002. V. C66. P. 054310.

15. National Nuclear Data Center, Brookhaven National Laboratory, http://www.nndc.bnl.gov/

16. *Soloviev V. G.* Theory of Atomic Nuclei: Quasiparticles and Phonons. Institute of Physics Publishing, Bristol and Philadelphia, 1992. 352 p.

17. *Izosimov I. N., Kalinnikov V. G., Myakushin M. Yu., Rimski-Korsakov A. A., Solnyshkin A. A., Suhonen J., Toivanen J.* Structure of the β^+/EC Decay Strength Function of ^{147g}Tb ($T_{1/2} \approx 1.6$ h) // J. Phys. G: Nucl. Part. Phys. 1998. V. 24. P. 831–845.

Received on May 22, 2017.

Редактор *Е. И. Крупко*

Подписано в печать 31.07.2017.
Формат 60 × 90/16. Бумага офсетная. Печать офсетная.
Усл. печ. л. 1,31. Уч.-изд. л. 1,76. Тираж 195 экз. Заказ № 59210.

Издательский отдел Объединенного института ядерных исследований
141980, г. Дубна, Московская обл., ул. Жолио-Кюри, 6.
E-mail: publish@jinr.ru
www.jinr.ru/publish/